Facile Synthesis of Ge-MWCNTs Nanocomposite Electrodes for High Capacity Lithium Ion Batteries

Subrahmanyam Goriparti[1,2], Umair Gulzar[1,2], Ermanno Miele[1], Francisco Palazon[3], Alice Scarpellini[3], Sergio Marras[3], Simone Monaco[3], Remo Proietti Zaccaria[1,4] and Claudio Capiglia[1,5]*

[1] Department of Nanostructures, Istituto Italiano di Tecnologia, Via Morego-30, Genova-16163 Italy

[2] Department of Physics, University of Genoa, Via Dodecaneso-33, Genova-16146, Italy

[3] Department of NanoChemistry, Istituto Italiano di Tecnologia, Via Morego-30, Genova-16163 Italy

[4] Cixi Institute of Biomedical Engineering, Ningbo Institute of Materials Technology and Engineering, Chinese Academy of Sciences, Zhejiang 315201, P. R. China

[5] Recruit R&D. Co., Ltd Ginza 8, Bldg., 8-4-17, Ginza, Chuo-ku, Tokyo, 104-8001, Japan

Corresponding author: claudio@mvc.biglobe.ne.jp

Supporting Information

Synthesis: The synthesis of Ge nanocrystal in oleylamine (OA) via solvethermal approach is here reported, where OA acts as both reducing agent as well as stabilizer for Ge nanocrystals. In a typical synthesis, the desired amount of GeI_2 is dissolved in OA in an inert atmosphere and transferred to a teflon vessel equipped with stainless steel autoclave. At room temperature (close to 25 °C) the Ge precursor, upon dissolution in OA, turns into germanium amides or germanium amide-iodide mixed complexes[1] as shown in Equation 1. When the autoclave reaches the temperature of 230 °C, Ge nanocrystals nucleation occurs from the thermally activated disproportionation reaction of Ge amides and/or amide-iodide complexes to form Ge^0, together with Ge(IV) amide-iodide complex[2], as shown in Equation 2. Finally, after 6 hours of reaction without any change in temperature, the complete reduction of Ge amide-iodide complexes is reached, as seen in Equation 3. This process is confirmed by the characteristic colour change from yellow to brown due to formation and growth of Ge nanocrystals (Ge^0), which were stabilized by OA groups.

$$GeI_2 + xH_2NC_{18}H_{35} \longrightarrow Ge(N\,C_{18}H_{35})_2 + GeI_{(2-x)}(HN\,C_{18}H_{35}) \qquad \text{Eq.1}$$

$$Ge(N\,C_{18}H_{35})_2 + GeI_{(2-x)}(HN\,C_{18}H_{35}) \xrightarrow{\blacktriangle} Ge^0 + GeI_{(4-x)}(HN\,C_{18}H_{35}) + xC_{18}H_{35}NH_3I \qquad \text{Eq.2}$$

$$Ge(N\,C_{18}H_{35})_2 + GeI_{(2-x)}(HN\,C_{18}H_{35}) + GeI_{(4-x)}(HN\,C_{18}H_{35}) \xrightarrow[\text{6 hrs}]{\blacktriangle} Ge^0 + xC_{18}H_{35}NH_3I \qquad \text{Eq.3}$$

Raman spectroscopy: The existence of Ge and the graphitic nature of carbon from MWCNTs was confirmed also through Raman spectroscopy. The three spectra associated to the three samples made of Ge, Ge-MWCNTs and MWCNTs are displayed in Figure S1. Pristine MWCNTs (Figure S1 (i)) show two peaks at about 1561 cm^{-1} (G band) and 1342 cm^{-1} (D band) corresponding to the vibration of sp^2-bonded carbon atoms in a two-dimensional hexagonal lattice and due to defects/disorder in the hexagonal graphitic layers, respectively. The low intensity of the D band when compared to the G band, leading to less defects and disorder, suggests a high degree of graphitization, hence a better electrical conductivity. Whereas Raman spectrum of Ge-MWCNTs (Figure S1 (iii)) shows four peaks at 293 cm^{-1}, 1578 cm^{-1}, 1351 cm^{-1} and 1620 cm^{-1}. The peak at 293 cm^{-1} corresponds to Ge nanocrystals, indeed it well matches with the pristine Ge nanocrystals spectrum in Figure S1 (ii). The additional peak at 1620 cm^{-1} is associated to disorder/defects of D^* band due to the incorporation of Ge nanocrystals on the surface of MWCNTs[1]. The peak well matches the response obtained from systems formed by nanoparticles of iron and titanium based oxides, metals like silver, gold, palladium and platinum embedded on carbon nanotubes[3-5]. Interestingly, after the attachments of Ge nanocrystals on the surface of MWCNTs, the G and D bands were slightly shifted towards higher wave numbers of about ~17 cm^{-1} and ~10 cm^{-1}, respectively. This shift of both G and D bands and the appearance of the new disorder peak of D^* could be ascribed to the charge transfer effect between Ge nanocrystals and MWCNTs. These results clearly show that one-step synthesis of Ge-MWCNTs composite slightly increases the density of defects on the MWCNTs. The enhancing of defects and disorder is expected to improve

the interaction between Ge and MWCNTs, to the extent that Ge are preferentially attach to MWCNTs. This is in good agreement with HRTEM of Ge-MWCNTs (Figure 3d).

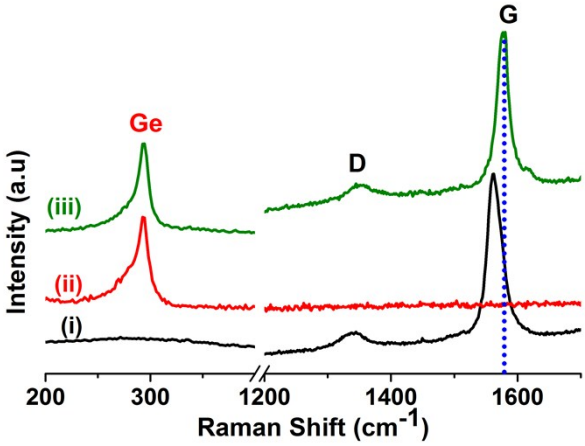

Figure S1. Raman spectra of (i) Ge nanocrystals, (ii) MWCNTs and (iii) Ge-MWCNTs.

Electrochemical analysis: In order to understand the specific role of MWCNTs and Ge from an electrochemical point of view, individual cells of Ge, MWCNTs and Ge-MWCNTs were fabricated and studied. Figure S2 shows the voltammograms of all the three cells in the potential range between 1.5 and 0.005 V *vs* Li/Li^+ at a scan rate of 0.02 mV s^{-1}. The cathodic (lithiation) and anodic (de-lithiation) profiles of Ge-MWCNTs exhibit multiple peaks, which are indicative of multi-step process of lithium redox reactions. In particular, these peaks can be separately associated to Ge and MWCNTs, where pristine Ge shows cathodic peaks at 0.32 V and 0.12 V, whereas MWCNTs shows redox peaks below 0.2 V. Similarly, the anodic (de-lithiation) scan of Ge-MWCNT composite shows five peaks, positioned at 0.09, 0.13, 0.50, 0.62 and 0.65 V, while the pristine Ge electrode displays two broad peaks at 0.51 V and 0.62 V. A slight difference in the lithium insertion and de-insertion response between Ge-MWCNTs nanocomposite electrode and pristine Ge or MWCNTs was observed. This difference may be related to the uniform distribution of Ge nanocrystals on the surface of electrically conductive MWCNTs and charge transfer interaction between Ge nanocrystals and MWCNTs (supported by slightly shift in Raman spectrum in Figure S1).

XRD of Ge nanocrystals:

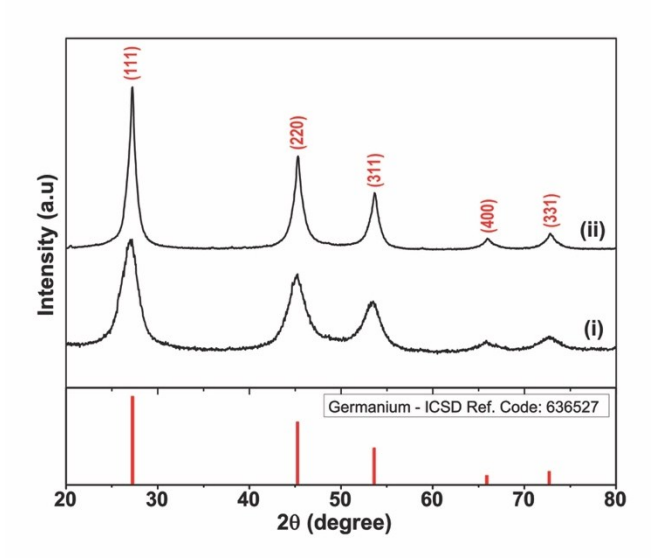

Figure S2. X-ray diffraction patterns of Ge nanocrystals (i) as synthesized and (ii) annealed at 500 °C.

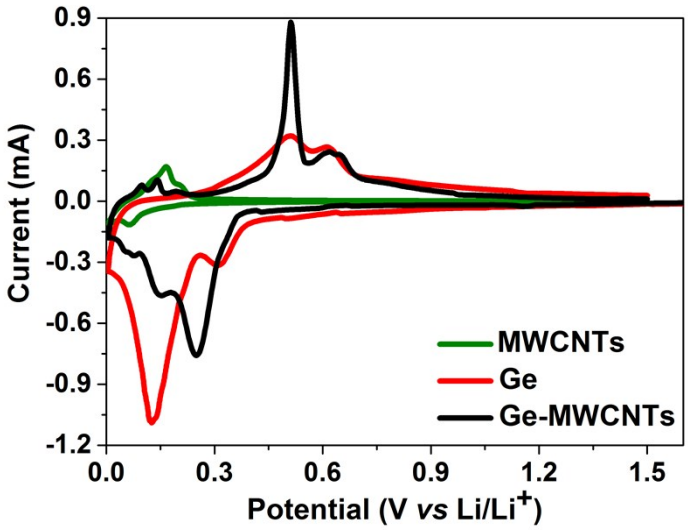

Figure S3. Cyclic voltammograms (first cycle) of Ge nanocrystals, Ge-MWCNTs nanocomposite and MWCNTs at the scan rate of 0.02 mV s^{-1}.

EDX and SEM:

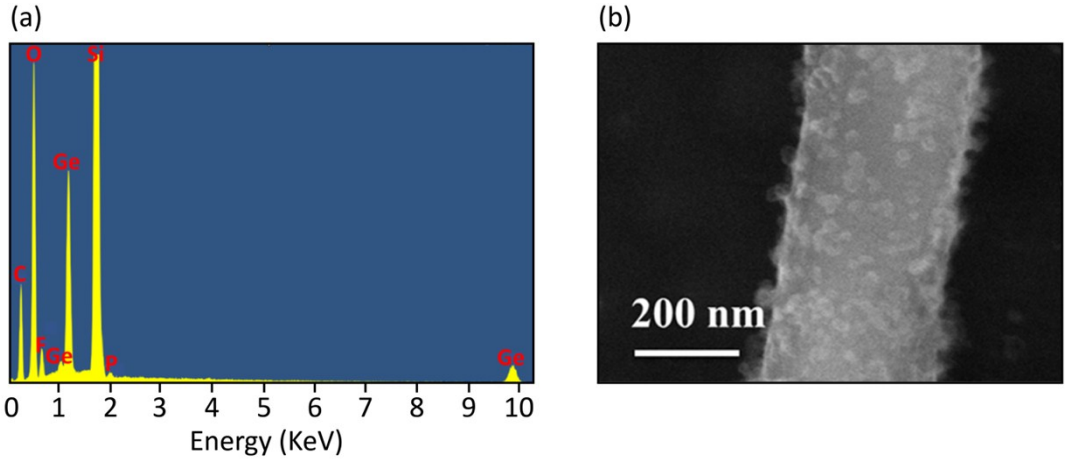

Figure S4. Energy dispersive X-ray spectroscopy of Ge-MWCNTs after five charge-discharge cycles (a) and their SEM image (b).

Electrochemical performance of Ge vs. Ge-MWCNTs composites:

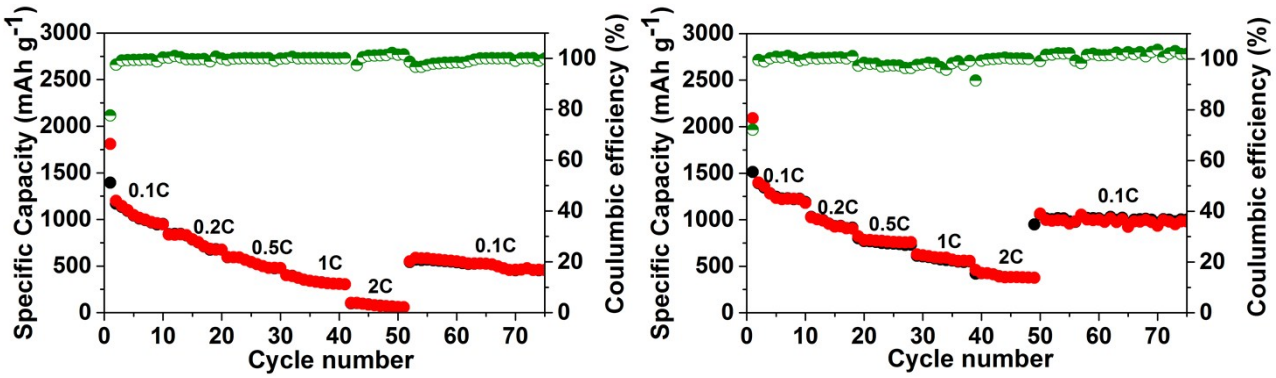

Figure S5. Galvanostatic charge-discharge capacities of (left) Ge, (right) Ge-MWCNTs at various current rates along with their columbic efficiencies.

Performance comparison:

Ge-Carbon composite	Synthesis process	Wt% of Ge	Capacity (mAh g^{-1})	Current rate (mA g^{-1})	No. of cycles	Ref.
Ge-C	Plasma	87.6	980	2000	100	6
Ge-Graphene	CVD	45.3	675	200	400	7
Ge@C/RGO	Solution method	~ 60	940	50	50	8
Ge-CNFs	Electrospinning	48.1	1420 829	~ 245 1624	100 250	9
Ge-carbon	Electrodeposition	-	972	160	50	10
Ge-MWCNTs	Thermal evaporation	~ 60-65	800	1623	200	11
Ge-N doped carbon	Sol-gel	68.5	1042	800	2000	12
Ge-MWCNTs	Solvothermal	80	1060 406	160 8000	60 400	Present article

Table 1S. Electrochemical properties of Ge and its carbon composites.

References

1. W. C. Johnson and A. E. Sidwell, *J. Am. Chem. Soc,* 1933, **55**, 1884-1889
2. D. A. Ruddy, J. C. Johnson, E. R. Smith, and N. R. Neale, *ACS Nano,* 2010, **4**, 7459-7466
3. A. M. O. de Zevallos-Márquez, M. J. S. P. Brasil, F. Iikawa, A. Abbaspourrad, C. Verissimo, S. A. Moshkalev and O. L. Alves, *J. Appl. Phys.*, 2010, **108**, 083501.
4. K. S. Subrahmanyam, A. K. Manna, S. K. Pati and C. N. R. Rao, *Chem. Phys. Lett.*, 2010, **497**, 70-75.
5. W. Zhang, V. Stolojan, S. R. P. Silva and C. W. Wu, *Spectrochim. Acta Part A: Molecul. Biomolecul. Spectroscopy*, 2014, **121**, 715-718.
6. W. Li, J. Zheng, T. Chen, T. Wang, X. Wang and X. Li, *Chem. Commun*, 2014, **50**, 2052-2054
7. J. Ren, Q. Wu, H. Tang, G. Hong, W. Zhang and S. Lee, *J. Mater. Chem. A*,2013, **1**, 1821-1821
8. D. Xue, S. Xin, Y. Yan, K. Jiang, Y. Yin, Y. Guo and L. Wan, *J. Am. Chem. Soc,* 2012, **134**, 2512-2515
9. W. Li, Z. Yang, J. Cheng, X. Zhong, L. Gub and Y. Yu, *Nanoscale*, 2014, **6**, 4532-4537
10. S. Kim, D. T. Ngo, J. Heo, C. Park and C. Park, *Electricmica Acta,* 2017, **238**, 319-329
11. I. Hwang, J. C. Kim, S. D. Seo, S. Lee, J. H. Lee and D.W. Kim, *Chem. Commun*, 2012, **48**, 7061-7063
12. X. Ma, Y. Zhou, M. Chen and L. Wu, Small, 2017, 13, 1700403